Nickel-Catalyzed Cross-Coupling of Photoredox-Generated Radicals: Uncovering a General Manifold for Stereoconvergence in Nickel-Catalyzed Cross-Couplings

Osvaldo Gutierrez, John C. Tellis, David N. Primer, Gary A. Molander,* and Marisa C. Kozlowski*

Department of Chemistry, Roy and Diana Vagelos Laboratories, University of Pennsylvania, Philadelphia, Pennsylvania 19104, United States

ⓢ *Supporting Information*

ABSTRACT: The cross-coupling of sp³-hybridized organoboron reagents via photoredox/nickel dual catalysis represents a new paradigm of reactivity for engaging alkylmetallic reagents in transition-metal-catalyzed processes. Reported here is an investigation into the mechanistic details of this important transformation using density functional theory. Calculations bring to light a new reaction pathway involving an alkylnickel(I) complex generated by addition of an alkyl radical to Ni(0) that is likely to operate simultaneously with the previously proposed mechanism. Analysis of the enantioselective variant of the transformation reveals an unexpected manifold for stereoinduction involving dynamic kinetic resolution (DKR) of a Ni(III) intermediate wherein the stereodetermining step is *reductive elimination*. Furthermore, calculations suggest that the DKR-based stereoinduction manifold may be responsible for stereoselectivity observed in numerous other stereoconvergent Ni-catalyzed cross-couplings and reductive couplings.

In the decades following their inception, transition-metal-catalyzed cross-coupling reactions (CCRs) have assumed a privileged role among methods for the construction of C−C bonds.[1] Although highly reliable for C(sp²)−C(sp²) couplings, significant limitations are often encountered in the application of sp³ hybridized reagents, particularly poorly nucleophilic secondary alkylborons. Here, slower rates of transmetalation often necessitate forcing conditions and/or harsh reagents (high temperatures, excess boronic acid, aqueous base), thereby limiting functional group tolerance while augmenting undesired side reactions, including protodeboronation, β-hydride elimination, and subsequent isomerization.[2]

In an effort to circumvent the challenges of transmetalation within the conventional catalytic regime, we recently reported a novel dual catalytic CCR in which the cooperative functions of an Ir photoredox catalyst and a Ni catalyst effect the cross-coupling of electronically activated potassium alkyltrifluoroborates with a variety of aryl bromides under exceptionally mild conditions (eq 1).[3] Most notably, the cross-coupling of a secondary benzylic trifluoroborate occurs stereoconvergently in the presence of a chiral ligand (eq 2), a stereochemical outcome that is unprecedented with boron reagents.[4]

We initially hypothesized a mechanistic scenario in which the Ni(0) catalyst **1** first engages the aryl bromide in oxidative
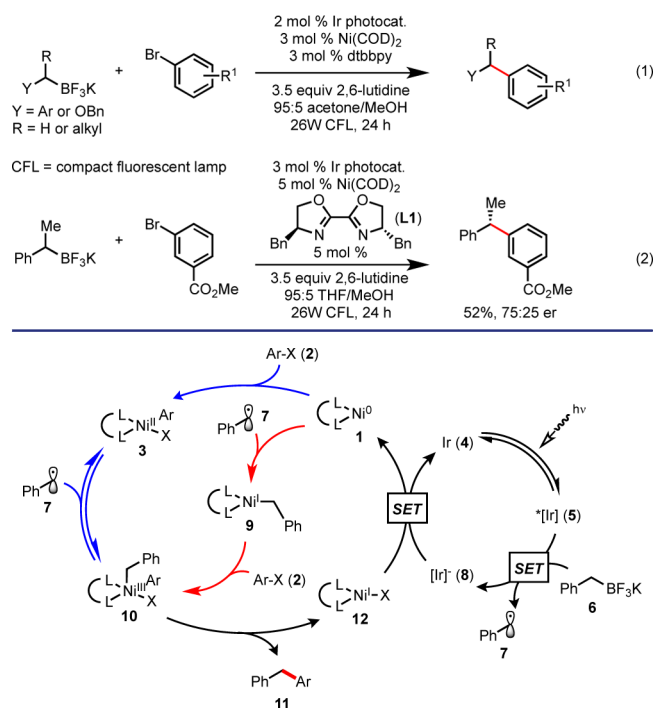

Figure 1. Initially proposed catalytic cycles (blue) and possible alternative indicated by computation (red) for photoredox/nickel dual catalytic CCR of potassium benzyltrifluoroborate and aryl bromides. Ir = Ir[dFCF₃ppy]₂(bpy)PF₆.

addition to afford arylnickel(II) complex **3** (Figure 1, blue). In parallel, oxidative fragmentation of an alkyltrifluoroborate **6** by the excited state of Ir photoredox catalyst **4** yields a C-centered radical that is rapidly captured by this Ni(II) complex. Reductive elimination from the resultant Ni(III) species **10** yields the cross-coupled product and Ni(I) complex **12**. Finally, single-electron reduction of Ni(I) by iridium complex **8** simultaneously regenerates the Ni(0) catalyst and the ground state photocatalyst. MacMillan, Doyle, and co-workers hypothesized a similar mechanistic scenario for the related cross-coupling of α-amino acids and *N,N*-dialkyl-*N*-arylamines with aryl halides.[5]

To understand more fully the mechanistic intricacies of this novel class of CCRs, we undertook a computational analysis of
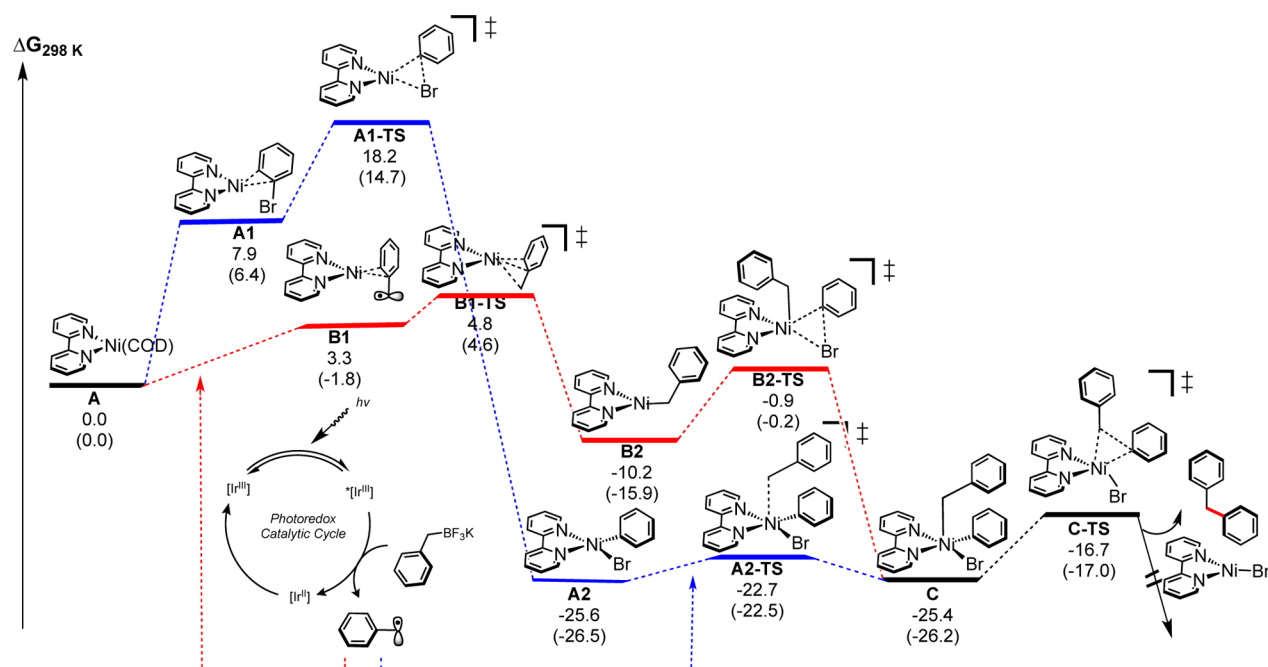
Figure 2. Reaction coordinate for the competing pathways using 2,2′-bipyridine. Relative Gibbs free energy values calculated with SMD-water-(U)M06/6-311+G(d,p)//UB3LYP/6-31G(d) and SMD-water-(U)M06/6-311+G(d,p)//UB3LYP/LANL2DZ (in parentheses).[12]

the Ni catalytic cycle. We were particularly interested in addressing two key questions: (1) To which oxidation state of Ni does the radical add? (2) Which step in the catalytic cycle is enantiodetermining? Importantly, although there have been numerous computational and experimental studies of traditional transition-metal-catalyzed CCRs,[6] there are limited computational analyses of Ni-catalyzed CCRs in which C-centered radicals and paramagnetic Ni species are invoked.[7] Herein, we report a detailed density functional theory (DFT) study of the catalytic cross-coupling of alkyltrifluoroborates and aryl bromides via single-electron transmetalation. Results reveal that the final reductive elimination accounts for the origin of stereoinduction for this important transformation.[8] A stereochemical model is proposed and, for the first time, supported by experiments with a series of substituted aryl bromides. These mechanistic findings are proposed to have far-reaching implications related to other stereoconvergent CCRs.

We initiated our studies by calculating the Gibbs free energy profile with 2,2′-bipyridine as a model ligand for the 4,4′-dtbbpy ligand used experimentally (Figure 2). Because of the presence of radicals and low-spin Ni intermediates, all optimizations were performed using a spin-unrestricted broken-symmetry UB3LYP functional with both the LANL2DZ and 6-31G(d) basis sets (with the Guess=mix keyword as implemented in Gaussian09).[9] Multiple spin states were considered for all intermediates and transition states. This method has been used before to rationalize selectivities accurately,[10] model radical Ni systems,[7a,b] and account for changes associated with ligands.[11] Single-point energy calculations of optimized structures were carried out in water (SMD solvation model) at the (U)M06/6-311+G(d,p) level of theory. For comparison, we computed the energetic profile by varying the basis set [6-311+G(d,p) for C, N, O, Br, H and SDD for Ni] and solvent (SMD in acetone), which showed similar energetics (see Supporting Information). Exhaustive conformational searches were performed for all intermediates to map out the lowest energy profile, and intrinsic reaction

coordinate (IRC) calculations were undertaken to ensure transitions states connected the illustrated ground states.

Beginning from square planar Ni(bpy)(COD) **A**, dissociation of 1,5,-cyclooctadiene (COD) and complexation to bromobenzene is energetically disfavored by 6–8 kcal/mol (Figure 2). However, oxidative addition is energetically feasible (15–18 kcal/mol) leading to square planar Ni(II) intermediate **A2**, which is ∼26 kcal/mol downhill in energy. The Ni(II)-to-Ni(III) process, occurring via addition of a benzyl radical (presumably generated in the concomitant photocatalytic cycle[3,5] from Figure 1), is found to *proceed via a low barrier (∼4 kcal/mol) transition state* **A2-TS** *and is reversible*. Significantly, the reductive elimination transition state (**C-TS**) leading to the CCR product and Ni(bpy)Br intermediate is ∼6 kcal/mol *higher* in energy than the radical addition/dissociation.

In an alternative mechanistic pathway, the Ni catalytic cycle can proceed via an alkylnickel(I) intermediate preceding oxidative addition (Figure 2 red). Ligand dissociation and radical η^2-complexation to Ni(0) leads to intermediate **B1**, which proceeds via a ∼5 kcal/mol energy barrier to form benzylnickel-(I) intermediate **B2**, a process that is favorable by ∼10–15 kcal/mol. This Ni(I) intermediate can undergo facile and irreversible oxidative addition (via **B2-TS**) to merge the two energetically feasible pathways via the pentacoordinated Ni(III) intermediate **C**. This result implies that, depending on the concentration of Ni(0) or Ni(II), both pathways can occur. Irrespective of the specific pathway, the dual photoredox/cross-coupling cycle *converges onto a Ni(III) intermediate that can dissociate the stabilized radical to form Ni(II) more rapidly than undergoing reductive elimination!* Subsequent reduction by the photoredox cycle will generate the Ni(0) intermediate to restart the catalytic cycle (Figure 1).

In our recent report, we observed modest enantioselectivity (75:25 er) with the use of chiral 4,4′-dibenzyl-2,2′-bis(2-oxazoline) ligand, **L1** (eq 2). We had previously suggested that the origin of enantioselectivity in the single-electron transmetalation of secondary alkyltrifluoroborates arises from facial
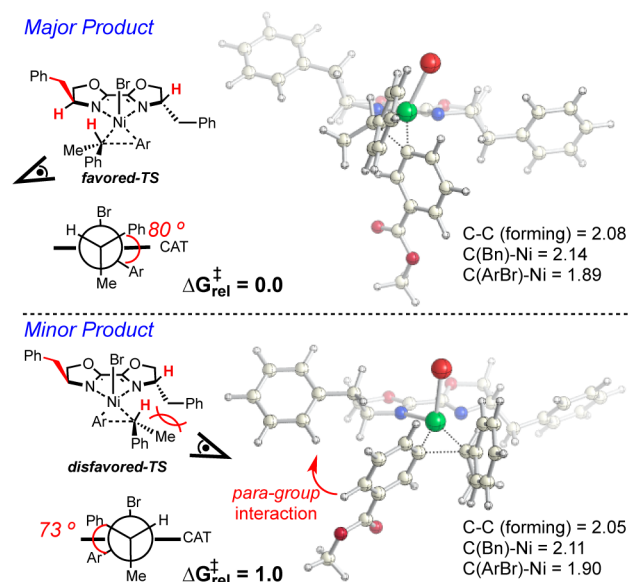
Figure 3. Competing diastereomeric transition states in the reductive elimination. Relative free energies (kcal/mol) are computed using SMD-water-(U)M06/6-311+G(d,p)//UB3LYP/6-31G(d).

Figure 4. Predicted and experimental reaction enantioselectivities.[17]

|			
	15a CN	**15b** Me	**15c** t-Bu
Exp:	57% ee	62 % ee	65 % ee
Calc:	54% ee	74% ee	84% ee

selectivity in the addition of the prochiral radical to the ligated Ni(II) center, followed by stereoretentive reductive elimination. However, if homolytic equilibration of the Ni(III)/Ni(II) pair is faster than reductive elimination, as these calculations indicate, then the origin of stereoselectivity should be found in the reductive elimination step.[7a] Thus, we propose that enantio-selectivity arises from a process best described as a dynamic kinetic resolution (DKR)[13] of Ni(III) complex **C′**.[14] In other words, addition of the secondary radical to the Ni center operates under Curtin-Hammett conditions[15] furnishing two equilibrating diastereomeric Ni(III) complexes, one of which reductively eliminates at a faster rate, leading to the major enantiomer. Stereoconvergence then results via stereochemical scrambling of the secondary alkyl subunit through dissociation and recombination. Indeed, computations of the diastereomeric transition states **C′** corresponding to eq 2 correlate well with experiment;[16] specifically, a Boltzmann distribution from calculated free energies of the eight lowest energy diastereomeric transition states predicts a 68% ee vs the experimental 50% ee. Examination of the structures reveals that the α-methylbenzyl group rotates to avoid gauche-like interactions along the forming C−C bond (Figure 3). In the lower energy diastereomeric transition state these interactions are minimized.

Having established reductive elimination as the enantio-determining step in these systems, other potential substrates were probed with the aim of establishing a correlation between the calculated and experimental selectivities. Calculations of the diastereomeric transition states for several substrates suggested that substituents at the *para*-position of the aryl bromide could enhance the enantioselectivity. In particular, larger *para*-substituents encounter steric interactions with the ligand benzyl group in the transition state leading to the minor enantiomeric product (see bottom structure in Figure 3). Notably, the stereochemical influence of these substituents distal from the bond-forming site would not be evident in the absence of this computational model. Gratifyingly, these predictions correlated well with experiment and afforded improved enantioselectivity in generating 1,1-diarylethane **15** (Figure 4).
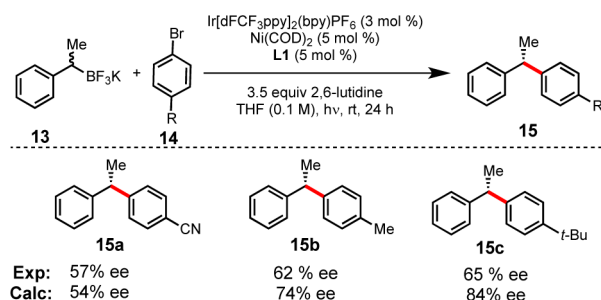
Moving forward, we became curious whether this DKR-controlled enantioselectivity operates in other asymmetric Ni-catalyzed cross-coupling processes. Of particular interest are reports documenting Ni-catalyzed asymmetric cross-couplings (Suzuki, Negishi, Hiyama, and Kumada)[18] and reductive cross-couplings.[19] Importantly, it can be argued that the "black box" nature of these transformations have limited their widespread development and adaptation, as no general model for stereo-induction has yet been proposed despite the large number of processes reported to date. Although a number of these asymmetric cross-couplings employ alkyl groups that would be precursors to stabilized radicals (i.e., benzylic, allylic, α-carbonyl, etc.), several examples of asymmetric cross-couplings of electronically unactivated alkyl subunits have been reported.[20] Although the analogy of the former examples to that reported here is readily apparent, it was less clear whether the proposed Ni(III) DKR manifold would be viable for systems in which less stable (e.g., unstabilized secondary alkyl) radicals were generated via homolysis of the Ni(III) intermediate. In an effort to address this question, the stereoconvergent cross-coupling of unactivated secondary alkyl bromides and primary alkylboranes reported by Fu and co-workers (eq 3)[20e] was examined computationally.
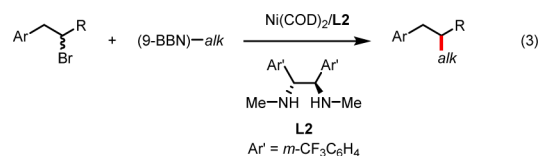
Beginning from the putative Ni(III) complex, the transition states for homolysis of the secondary alkyl substituent and C−C bond-forming reductive elimination were computed. As shown in Figure 5, these calculations convincingly support a scenario analogous to that described above; that is, Ni(III) complex **10a** exists in homolytic equilibrium with Ni(II) complex **3a** and the free alkyl radical in a process that is much faster than the subsequent reductive elimination leading to Ni(I) complex **12a** and cross-coupled alkane product. As such, *we propose that*
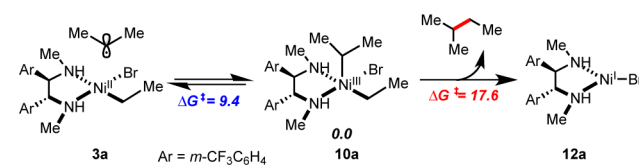
Figure 5. Energy barriers for the competing unstabilized alkyl radical dissociation and reductive elimination transition states with chiral diamine ligand **L2**. Relative free energies (kcal/mol) are computed using SMD-water-(U)M06/6-311+G(d,p)//B3LYP/6-31G(d) in SMD (water) level of theory.

stereoconvergence in these processes occurs by the same Ni(III) DKR process that we have elucidated for photoredox/nickel dual catalytic organoboron cross-coupling. This newfound knowledge regarding the fundamental origin of enantioinduction in Ni-catalyzed stereoconvergent processes can be used to augment stereoselectivity in known transformations through rational design and may be helpful in identifying new substrate classes that can participate via this manifold. These results are in agreement with the lack of products with long-lived radical intermediates. Specifically, radicals that quickly and favorably complex to the Ni center as proposed in Figure 2 avoid radical pathways such as cyclization by a pendant alkene. We are currently investigating the full scope of this proposal for various Ni-catalyzed C−C bond-forming processes involving alkyl radical intermediates, including the factors that might change the enantiodetermining step.

In summary, we have employed DFT calculations to investigate the reaction pathway of the nickel/photoredox dual catalytic cross-coupling of aryl bromides with C-centered radicals derived from alkyltrifluoroborates. These computations suggest a mechanistic scenario wherein the radical can enter the cross-coupling cycle by addition to either Ni(0) or Ni(II).[21] The two pathways converge upon a common Ni(III) intermediate that is able to release the stabilized alkyl radical via Ni−C bond homolysis, thus establishing an unexpected equilibrium between this high valent Ni(III) and the Ni(II)/radical pair. The cross-coupled product is then generated via irreversible reductive elimination. The reductive elimination barrier was computed to be significantly higher in energy than the barrier associated with the reversible homolysis process. Calculations show that the stereoinduction occurs through DKR of the Ni(III) intermediate according to the Curtin−Hammett principle. Experimental results have offered support for the proposed stereochemical model. Most importantly, the Curtin−Hammett DKR stereoinduction model appears to be broadly operative in various related stereoconvergent Ni-catalyzed processes,[7,18] offering a rationalization for the mechanism of stereoselectivity in these transformations for the first time.

■ ASSOCIATED CONTENT

Ⓢ Supporting Information

Computational and experimental details; complete ref 9. This material is available free of charge via the Internet at http://pubs.acs.org.

■ AUTHOR INFORMATION

Corresponding Authors
*gmolandr@sas.upenn.edu
*marisa@sas.upenn.edu

Notes
The authors declare no competing financial interest.

■ ACKNOWLEDGMENTS

■ REFERENCES

(1) *Metal-Catalyzed Cross-Coupling Reactions*; de Meijere, A., Diederich, F., Eds.; Wiley-VCH: Weinheim, Germany, 2004.

(2) Hartwig, J. F. *Organotransition Metal Chemistry: From Bonding to Catalysis*, 3rd ed.; University Science: Sausalito, CA, 2010.

(3) (a) Tellis, J. C.; Primer, D. N.; Molander, G. A. *Science* **2014**, *345*, 433. (b) Primer, D. N.; Karakaya, I.; Tellis, J. C.; Molander, G. A. *J. Am. Chem. Soc.* **2015**, *137*, 2195.

(4) (a) Li, L.; Wang, C. Y.; Huang, R.; Biscoe, M. R. *Nature Chem.* **2013**, *5*, 607. (b) Li, L.; Zhao, S.; Joshi-Pangu, A.; Diane, M.; Biscoe, M. R. *J. Am. Chem. Soc.* **2014**, *136*, 14027.

(5) Zuo, Z.; Ahneman, D. T.; Chu, L.; Terret, J. A.; Doyle, A. G.; MacMillan, D. W. C. *Science* **2014**, *345*, 437.

(6) Ananikov, V. P., Ed. *Understanding Organometallic Reaction Mechanisms and Catalysis*; Wiley-VCH: Weinheim, Germany, 2015.

(7) (a) Lin, X.; Sun, J.; Xi, Y.; Lin, D. *Organometallics* **2011**, *30*, 3284. (b) Lin, X.; Phillips, D. L. *J. Org. Chem.* **2008**, *73*, 3680. (c) Li, Z.; Jiang, Y.-Y.; Fu, Y. *Chem.—Eur. J.* **2012**, *18*, 4345. (d) Ren, Q.; Jiang, F.; Gong, H. *J. Organomet. Chem.* **2014**, *770*, 130.

(8) (a) Lloyd-Jones, G. C.; Ball, L. T. *Science* **2014**, *345*, 381. (b) Leonori, D.; Varinder K; Aggarwal, V. K. *Angew. Chem., Int. Ed.* **2014**, *54*, 1082.

(9) Frisch, M. J.; et al. *Gaussian 09*, rev C.01; Gaussian, Inc.: Wallingford, CT, 2009.

(10) Um, J. M.; Gutierrez, O.; Schoenebeck, F.; Houk, K. N.; MacMillan, D. W. C. *J. Am. Chem. Soc.* **2010**, *132*, 6001.

(11) (a) Uyeda, C.; Peters, J. C. *Chem. Sci.* **2013**, *4*, 157. (b) Nomura, M.; Cauchy, T.; Geoffroy, M.; Adkine, P.; Fourmigué, M. *Inorg. Chem.* **2006**, *45*, 8194. (c) Jones, G. D.; Martin, J. L.; McFarland, C.; Allen, O. R.; Hall, R. E.; Haley, A. D.; Brandon, R. J.; Konovalova, T.; Desrochers, P. J.; Pulay, P.; Vicic, D. A. *J. Am. Chem. Soc.* **2006**, *128*, 13175.

(12) M06-2X/6-311+G(d,p)-solvated single-point calculations using B3LYP geometries are more effective than B3LYP alone in estimating absolute reaction barriers. See: Krenske, E. H.; Agopcan, S.; Aviyente, V.; Houk, K. N.; Johnson, B. A.; Holmes, A. B. *J. Am. Chem. Soc.* **2012**, *134*, 12010.

(13) Beak, P.; Basu, A.; Gallagher, D. J.; Park, Y.-S.; Thayumanavan, S. *Acc. Chem. Res.* **1996**, *29*, 552.

(14) Reaction of (*R*)-1-phenylethyltrifluoroborate using chiral ligand **L1** resulted in enantioselectivity indistinguishable from that observed using racemic substrate. Reaction of the enantioenriched trifluoroborate with an achiral ligand produced racemic product (see Supporting Information). These results rule out a classical kinetic resolution for this process.

(15) (a) Seeman, J. I. *J. Chem. Ed.* **1986**, *63*, 42. (b) Seeman, J. I. *Chem. Rev.* **1983**, *83*, 84.

(16) Preliminary calculations of A2-TS′ corresponding to eq 2 reveal a conformer 2 kcal/mol lower in energy than the lowest energy C-TS′.

(17) Calculated ratios were computed using the lowest two diastereomeric transition states computed using SMD-water-UM06/6-311+G(d,p)//UB3LYP/6-31G(d).

(18) For reviews on secondary alkyl halides in Ni-catalyzed cross-coupling, including stereoconvergent examples, see: (a) Tasker, S. Z.; Standley, E. A.; Jamison, T. F. *Nature* **2014**, *509*, 299. (b) Rudolph, A.; Lautens, M. *Angew. Chem., Int. Ed.* **2009**, *48*, 2656.

(19) (a) Cherney, A. H.; Reisman, S. E. *J. Am. Chem. Soc.* **2014**, *136*, 14365. (b) Cherney, A. H.; Kadunce, N. T.; Reisman, S. E. *J. Am. Chem. Soc.* **2013**, *135*, 7442.

(20) (a) Wilsily, A.; Tramutola, F.; Owston, N. A.; Fu, G. C. *J. Am. Chem. Soc.* **2012**, *134*, 5794. (b) Zultanski, S. L.; Fu, G. C. *J. Am. Chem. Soc.* **2011**, *133*, 15362. (c) Lu, Z.; Wilsily, A.; Fu, G. C. *J. Am. Chem. Soc.* **2011**, *133*, 8154. (d) Owston, N. A.; Fu, G. C. *J. Am. Chem. Soc.* **2010**, *132*, 11908. (e) Saito, B.; Fu, G. C. *J. Am. Chem. Soc.* **2008**, *130*, 6694. (f) Jiang, X.; Sakthivel, S.; Kulbitski, K.; Nisnevich, G.; Gandelman, M. *J. Am. Chem. Soc.* **2014**, *136*, 9548.

(21) For a recent report on Ni(II) intermediates in the related Negishi coupling, see: Schley, N. D.; Fu, G. C. *J. Am. Chem. Soc.* **2014**, *136*, 16588.